Wang *et al. Chin. J. Mech. Eng.* (2020) 33:83
https://doi.org/10.1186/s10033-020-00502-x

Chinese Journal of Mechanical Engineering

ORIGINAL ARTICLE

Open Access

Amending Research on the Expression of the Contact Force of the Spindle Barrel Finishing Based on EDEM Simulation

Na Wang[1,2], Shengqiang Yang[1,2*], Tingting Zhao[1], Bo Cao[1,2] and Chengwei Wang[1,2]

Abstract

The spindle barrel finishing is commonly used to improve the surface integrity of the important parts of the high-end equipment while it is difficult to provide enough test artifacts for the traditional trial and error experiment to obtain the desirable processing technology. The EDEM simulation of the spindle barrel finishing can provide effective help for the process design, however, the difference between the simulation and experiment is closely related to the selection of the contact model during simulation. In this paper, simulations and experiments are conducted based on the identical apparatus and conditions to facilitate the comparison and validation between each other. Based on the Hertz contact theory, the effect of the material properties of contact objects and the relative position of the workpiece on the contact force is qualified. The expression of the correlation coefficient of the contact model is deduced. Then the formula for calculating the contact force between the barrel finishing abrasive and the workpiece that includes influence coefficient of the material properties and the relative positions is established. Finally, the contact force calculation formula is verified by changing the rotating speed. The result shows that the material correction coefficient ranges from 1.41 to 2.38, which is inversely related to the equivalent modulus E. The position correction coefficient ranges from 2.0 to 2.3. The relative error value between the calculation result and the experimental test result is from 0.58% to 14.07%. This research lay a theoretical foundation for the correction theory of the core elements of the spindle barrel finishing process.

Keywords: Spindle barrel finishing processing, EDEM simulation, Hertz-Mindlin (no slip) contact model, Average contact force, Modified coefficient

1 Introduction

Improving the surface quality of parts is one of the important ways to improve the performance, enhancing the reliability and extend the service life of products. The barrel finishing technology [1] is a basic manufacturing process technology in the field of mechanical processing. It aims to improve the surface quality of parts and ameliorate the surface integrity of parts, which belongs to the category of precision and ultra-precision machining. The barrel finishing process is widely used due to the wide application scope [2–4], good processing effect [5, 6], low processing cost and friendly processing environment [7, 8]. Cariapa [9] points out that the barrel finishing process is used to improve the surface quality of almost 50% machined parts in the world.

The barrel finishing process is a complex system. Several factors needs to be considered at the same time, including the processing objects and requirements, the machining equipment and parameters, the type and shape and size of the barrel finishing abrasive, and the chemical agents etc. There has been rapidly growing interest in the research of the barrel finishing process. The traditional trial and error experiment to obtain the desirable processing technology cannot meet the requirements of the rapid development. According to

*Correspondence: tutysq@263.net.cn
[1] College of Mechanical and Vehicle Engineering, Taiyuan University of Technology, Taiyuan 030024, China
Full list of author information is available at the end of the article

the characteristics of the barrel finishing process, adopting the DEM (discrete element simulation) technology to realize the process simulation can reduce or replace complicated process experiments, and the discrete element theory provides a great support to solve practical engineering problems [10–14]. Many practitioners use EDEM software for the numerical simulation of the barrel finishing process. It is difficult to calibrate the parameters of the DEM simulation, including the static friction coefficient, the sliding friction coefficient and the rolling friction coefficient [15, 16]. Due to the lack of the quantitative difference between the experiment and simulation results, it is difficult to design the process planning based on the DEM simulation.

The Hertz-Mindlin non-slip contact model is often used in the EDEM simulation of the barrel finishing process. Tian et al. [17] established the dynamic model of the crank barrel finishing, and considered the different processing mechanisms of the normal force and tangential force to carry out the simulation analysis of the crankshaft average contact force in the machining process. Yan et al. [18] simulated the grinding medium of the waterfall vibration finishing, and analyzed the change rule of the barrel finishing medium and the workpiece under different processing parameters. Song [19] carried out the theoretical analysis and simulation of the dynamic model of medium and workpiece in the process of centrifugal barrel finishing. Chen [20] carried out the numerical simulation and theoretical analysis on the basis of theoretical analysis of the horizontal centrifugal barrel finishing medium. Li et al. [21] performed theoretical and simulation analysis on the movement mechanism and the distribution characteristics of medium in the centrifugal barrel finishing. They all selected the Hertz-Mindlin non-slip contact model in the EDEM software system, while the rationality of the contact model were not analyzed and verified. Nowadays, the spindle barrel finishing process is mostly employed to improve the surface quality of precious parts in high-end devices manufacturing. During the processing, the workpiece is clamped and fixed on the rotary spindle. The workpiece is located into a roller that performs a rotary motion and is filled with a certain amount of barrel finishing abrasive. The spindle of the workpiece is parallel to the main axis of the roller and maintains an appropriate distance. The surface quality and integrity of the parts is improved by the micro grinding effects caused by the collisions, rolling, sliding and scratching between the barrel finishing media and the workpieces.

In this paper, the spindle barrel finishing is analyzed by both experiment and simulations based on the identical apparatus and conditions to facilitate the comparison and validation between each other. The dry spherical particles are selected as the processing medium. The Hertz-Mindlin (no slip) contact model is used in the simulation, the error of the frontal contact force between the workpiece and the barrel finishing abrasive in the numerical simulation and experimental is analyzed. Based on the Hertz collision contact, the effect of the material properties of contact objects and the relative position of workpiece on the contact force is qualified, the expression of the correction coefficient of the contact model is deduced. The formula for calculating the contact force between the barrel finishing abrasive and the workpiece is established, which can provide a credible calculation method for the barrel finishing process.

2 Experiment and Simulation

2.1 Experimental Test

The experiment is based on the actual spindle barrel finishing equipment. The spindle is fixed during processing, taking into account, the reliability of the pressure sensor signal transmission and the purpose of the experiment is to test the front contact force between the workpiece and the barrel finishing abrasive. The sensor position is adjusted up and down by two inner and outer steel tubes with 15 mm and 30 mm diameter respectively, and the sensor is fixed on the outer wall of the inner tube (the workpiece is fixed with sensor inner tube in the text). The transmission line is connected in the inner tube to reduce vibration. This device can ensure the stability of the transmission of the data.

To make the environment of the experimental test consistent with the environment of simulation, the experiment process parameters are built by considering the calculation efficiency of the EDEM software. The experimental equipment device diagram is shown in Figure 1. The rotary drum is a 201 stainless steel (0Cr18Ni9 (GB)) roller with the diameter of 216 mm and the height of 210 mm.

The processing medium is the dry finishing abrasive of the corundum spherical (as shown in Figure 2) with an average diameter of $D=6.2044$ mm (standard deviation S.D. $=0.0504$, sample number is 80) and the loading capacity is 60% of the roller volume.

The contact force between the barrel finishing abrasive and the workpiece is acquired with the help of the dynamic force sensor with model 501F01 (Beijing Yiyang Stress Vibration Testing Technology Co., Ltd.), the DH5902 robust data acquisition system (Jiangsu Donghua Testing Technology Co., Ltd.) and the computer.

A rectangular coordinate system is established by taking the center axis of the roller as the z axis and the bottom surface of the roller as the xOy plane as shown in Figure 3.

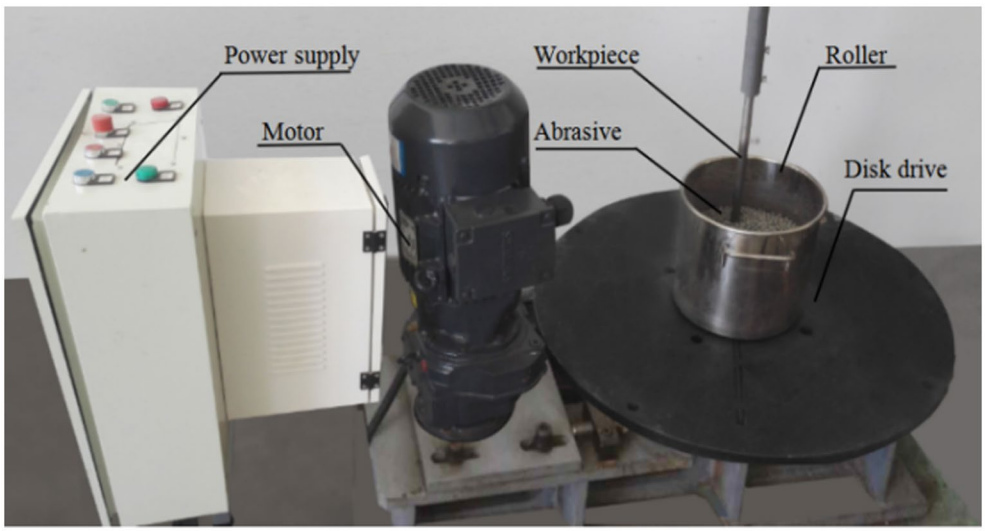

Figure 1. Diagram of the experimental equipment device

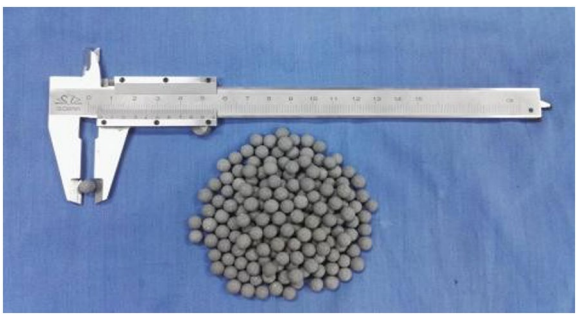

Figure 2. Barrel finishing abrasive

Figure 3. Schematic diagram of sampling points location

Set the dynamic force sensor sensitivity to 10.0 mV/N, test range to 50 N, and sampling frequency to 5000 Hz. And 20 different sampling point locations on the *xOz* plane are selected, which the coordinates are shown in Table 1. During the experiment, keep the front surface of the sensor always coplanar with the central axis of the roller and test the frontal contact force between the barrel finishing abrasive and the workpiece. Each sampling point is tested for three times. Figure 4 is the schematic diagram of the dynamic force testing device.

Considering the effect of the noise on the experimental data during the experiment, we use the haar operator to perform wavelet noise reduction on the signal image after the test. For example, the distance of the workpiece from the center axis is $x=70$ mm and the distance from the bottom of the roller is $z=70$ mm, when the roller rotation speed reaches 100 rpm, the reconstructed signal after the denoised signal by a 2 stage haar wavelet are shown in the Figure 5. The Figure 5 shows the comparison between the original signal and the denoised signal of contact force of workpiece, the signal contact force after denoised is much smaller than the original signal contact force. The piezo-electric sensor surface will deform after being subjected the force of the barrel finishing abrasive. Press the sensor lightly before the test, to check the sensors positive and negative pressure output value. It is found that the sensor transmits a negative pressure value after the compression and the positive force is the elasticity restoring force of the sensor surface during unloading. It deals with the contact force test value after denoised and eliminates the positive pressure value according to

Table 1. Coordinate of the sampling points

Points	**A**	**B**	**C**	**D**	**E**
x (mm)	40	55	70	85	40
z (mm)	115	115	115	115	100
Points	**F**	**G**	**H**	**I**	**J**
x (mm)	55	70	85	40	55
z (mm)	100	100	100	85	85
Points	**K**	**L**	**M**	**N**	**O**
x (mm)	70	85	40	55	70
z (mm)	85	85	70	70	70
Points	**P**	**Q**	**R**	**S**	**T**
x (mm)	85	40	55	70	85
z (mm)	70	55	55	55	55

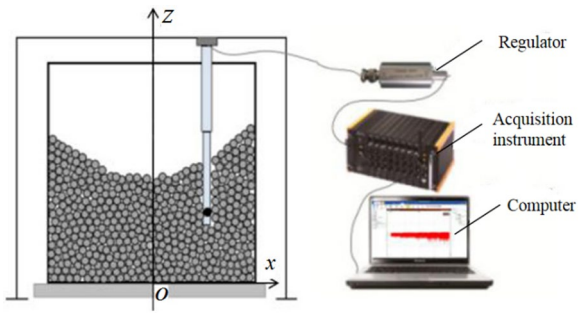

Figure 4. Schematic diagram of dynamic force test device

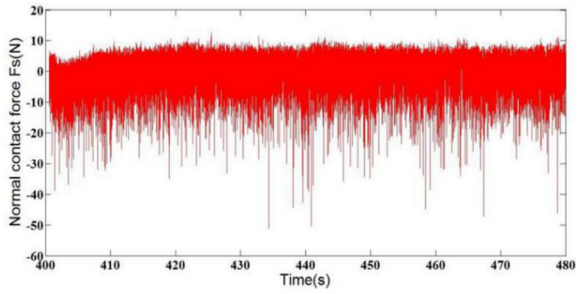

a The original signal

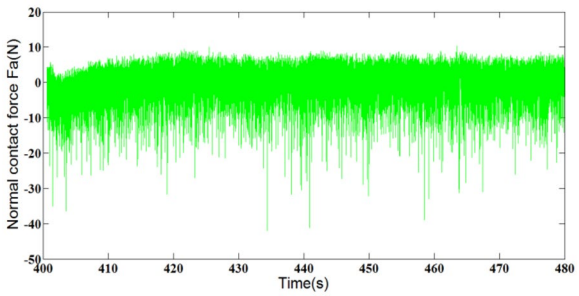

b The denoised signal

Figure 5. Comparison between the original and denoised signal

the characteristics of the sensor itself, and just holds the negative pressure value and calculates the mean force. Table 2 indicates the average contact force of each sampling point at the front of the workpiece.

2.2 Simulation

The Hertz-Mindlin (no-slip) contact model is used in the simulation with EDEM. In a normal distribution set the spherical particles is $R=3$ mm. Import the geometric model, then establish the granule factory and set the amount of the dynamically generated particles as 22000, which is generated from $t=0$ and at the rate of 10000 per second. The initial fall velocity is -2 m/s; set the roller to rotate from $t=2.2$ s and the speed is 100 r/min; set the time step as 30% of Rayleigh time, and the simulation time as 5 s, and the mesh size as $2R_{\min}$.

The material parameters of the roller, the barrel finishing abrasive and the workpiece are shown in Table 3. The related physical performance parameters between the geometries are shown in Table 4. Among them, the magnitude of the restitution coefficient depend not only on the quality of the material itself, but also on the relative velocity between the contact bodies. Previous study reveals that most of authors choose the restitution coefficient is 0.9 [22, 23], while studying the low-velocity collisions. Having learned from the domestic and foreign scholars on the value of rebound coefficient, this paper selects the restitution coefficient between all contact materials is 0.9.

The static friction coefficient and the coefficient of rolling friction are calibrated through the stacking angle experiment. To obtain the model of stacking

Table 2. Experimental results of average contact force of the workpiece at $v=100$ r/min at different positions F(N)

Z (mm)	*x* (mm)			
	40	**55**	**70**	**85**
55	2.3562	3.5821	4.9652	6.0252
70	1.9642	2.9831	4.5137	5.5480
85	1.5623	2.3584	3.5157	4.2871
100	0.9440	1.3313	3.2175	3.0707
115	0.4824	0.9990	1.6628	3.0381

Table 3. The related material parameters

Material parameters	Poisson ratio	Density (g/cm^3)	Shear modulus (GPa)
0Cr18Ni9 (roller)	0.285	7.93	79.4
Brown corundum (abrasive)	0.21	2.675	124
0Cr18Ni13Si4 (workpiece)	0.27	7.86	77

Table 4. The related physical performance parameters

Correlation coefficient	Restitution	Static friction	Rolling friction
Abrasive-abrasive	0.9	0.45	0.05
Roller-abrasive	0.9	0.3	0.05
Workpiece-abrasive	0.9	0.3	0.05

angle regression, the multiple regression fitting analysis is performed first. Then, the measurement of variance is used to assess the important variables. Finally, the regression model is refined, allowing the simulation of the stacking angle experiment and achieving a high degree of similarity in the stacking angle and form, in order to obtain the optimal touch parameters.

The stacking angle simulation and the implementation phase of experiments [24] were performed as follows. Put a certain amount of abrasive into the lifting cylinder. After the abrasive are stationary in the cylinder, lift the cylinder slowly to make the abrasive flow out from the bottom of the cylinder and form an abrasive pile on the plate. After the abrasive pile is stable, measure the stacking angle of the abrasive pile. The sensitivity analysis is carried out on the basis of the DEM [8], and the process is mainly conducted by continuously adjusting the discrete element parameters of the finishing media to ensure that the media repose angle is the same as that in the experiment, so that the optimal solution is obtained. The experimental results are shown in Figure 6.

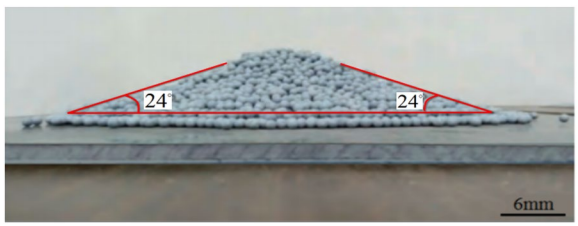

Figure 6. Experimental result of repose angles of barrel finishing abrasive

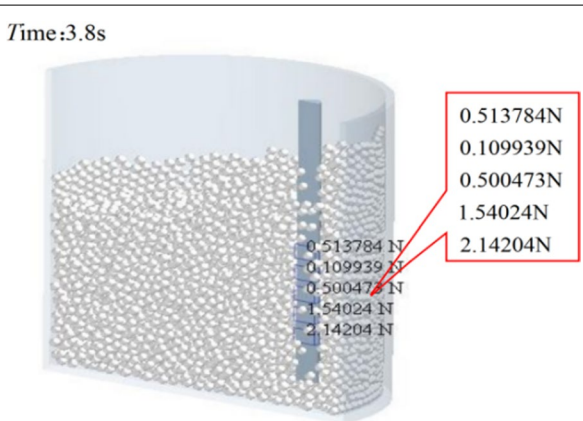

Figure 7. Distribution chart of grid location

Change the workpiece radial positions to multiple simulations. Once the simulation is complete, enter the EDEM's post-processing tool module to build five grids at different work piece axial position. The geometry of each grid is 15 mm × 4 mm × 10 mm. Taking the central axis $x=85$ mm as an example, Figure 7 shows the normal contact force at each mesh on the workpiece at $t=3.8$ s.

Figure 8 shows the normal contact force of the grids center where $z=55$ mm and $z=70$ mm at different moments at $x=70$mm. Export the average normal contact force between the barrel finishing abrasive and the workpiece at each contact position when the rotation speed is stabilized.

The center position of the grid and the normal contact force at each position are shown in Table 5.

2.3 Comparison of Experimental and Simulation

In the barrel finishing process, collision and compression predominate the frontal contact force between the barrel finishing abrasive and the workpiece [25]. The comparison results of the average normal contact force in the numerical simulation with the experimental test with the workpiece in different positions are shown in Figure 9.

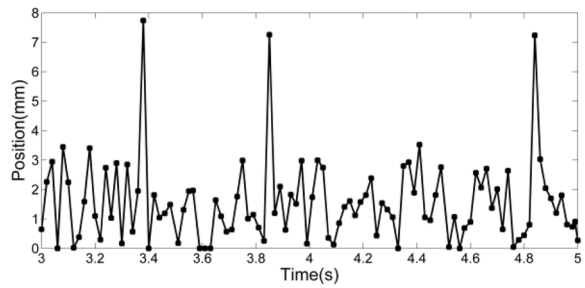

a z=55 mm

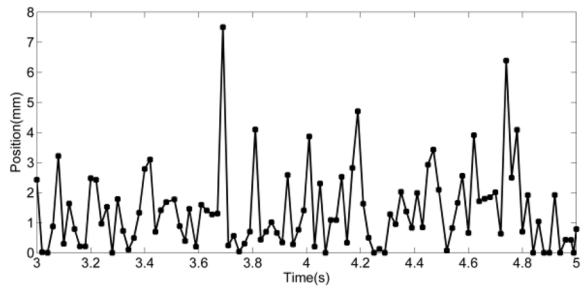

b z=70 mm

Figure 8. Normal contact force at different grids distance x=70 mm to the center axis

Table 5. Simulation result of the average contact force of the workpiece at different positions at v=100 r/min F(N)

z (mm)	x (mm)			
	40	55	70	85
55	0.7242	1.0036	1.5570	2.0001
70	0.5562	0.8599	1.3852	1.7368
85	0.3386	0.7020	1.1249	1.3708
100	0.2177	0.3919	1.1006	1.0056
115	0.1333	0.2815	0.5223	0.8218

As shown in Figure 9, it is found that the deeper the distance, the greater the contact force would be for the usual contact force in the axial and radial directions the farther away from the center of the roller is, the greater the contact force will be. This law applies to both the simulation and experimental results. Set the relative error of the average contact force between the simulation results and the experimental results as:

$$err = \left| \frac{F_e - F_s}{F_s} \right|, \tag{1}$$

where F_e is the experimental results; F_s is the simulation results.

Combining Tables 2 and 5, the relative error at each sampling point is shown in Figure 10 with the value from 66.8% to 72.4% by Eq. (1). Obviously, by using the Hertz-MD non-slip contact model in the simulation, a significant error occur, so it is important to modify the expression of the contact force between the bareel finishing abrasive and the workpiece based on the Hertz contact theory.

3 Theoretical Analysis

3.1 Hertz Contact Theory

The DEM is used to analyze the barrel finishing process in this paper. The contact force generated by the frontal collision between the barrel finishing abrasive and the workpiece is analyzed based on the Hertz contact theory.

The Hertz contact force [26] F_n can be obtained by Eqs. (2–4) as follows:

$$F_n = \frac{4}{3} E^* (R^*)^{1/2} \delta_n^{3/2}, \tag{2}$$

$$\frac{1}{E^*} = \left(\frac{1-\mu_1^2}{E_1} + \frac{1-\mu_2^2}{E_2} \right), \tag{3}$$

$$\frac{1}{R^*} = \frac{1}{R_1} + \frac{1}{R_2}. \tag{4}$$

In the formula, R^* is the equivalent particle radius, E^* is the equivalent modulus of elasticity, δ_n is the normal overlap quantity. E_1, E_2, μ_1, μ_2, R_1, R_2 respectively represent the elastic modulus, Poisson's ratio and the radius of the contact object. The radius of the flat surface can be considered as infinite when the particles are in contact with the plan.

3.2 Setting of the Yield Stress

Based on the Hertz contact theory, Brizme et al. [27] assumed that the processed workpiece material met the Mises yield criterion, and the initial yield stress p_y would obey the relationship of Eq. (5):

$$p_y = (1.234 + 1.256\mu)Y, \tag{5}$$

where μ and Y respectively indicate the Poisson's ratio and the yield strength of the processed workpiece material.

4 Qulification of Correction Coefficients

In fact, the surface of the workpiece has different degrees of deformation in the contact process between the barrel finishing abrasive and the workpiece. From the viewpoint of the energy conservation, different contact materials will lead to different degrees of deformation, meanwhile, the

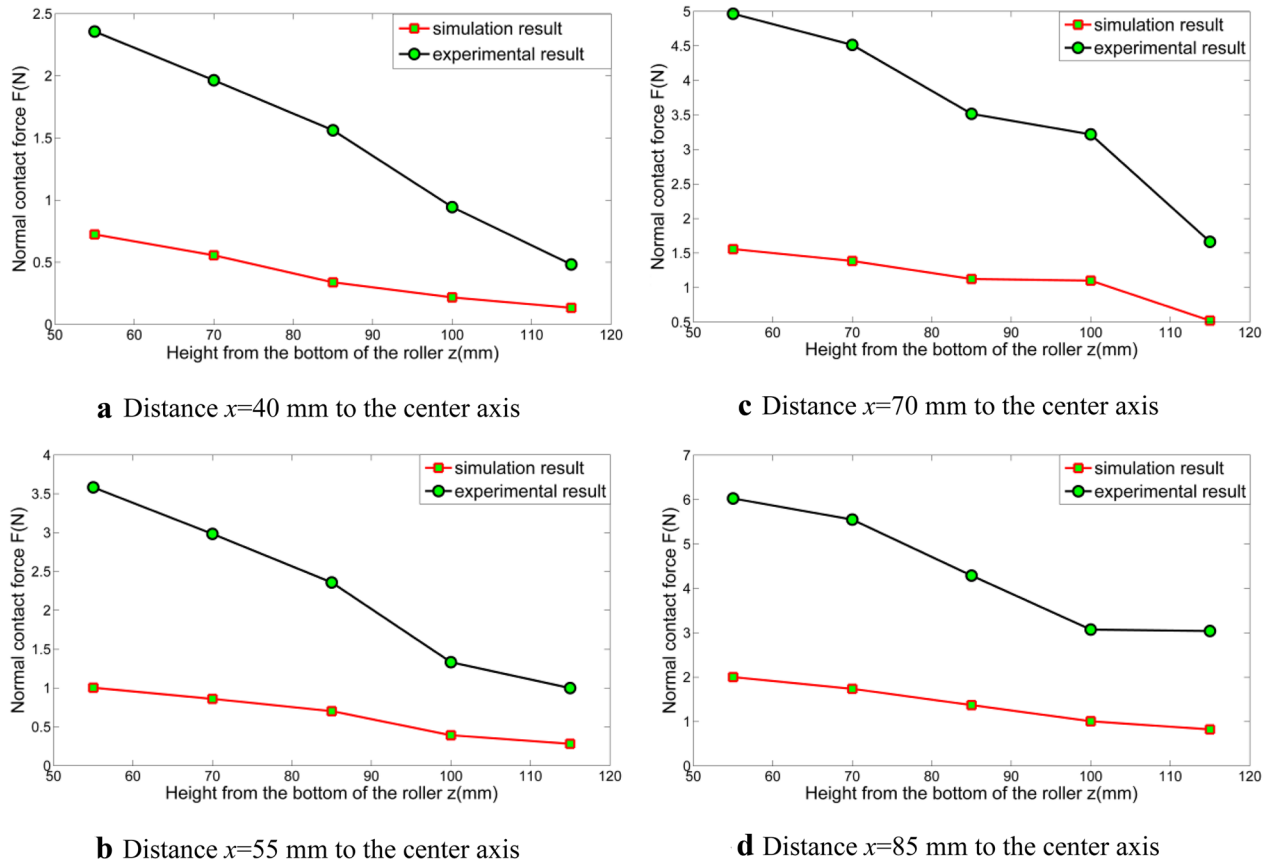

Figure 9. Comparison of simulation results and experimental results at different locations

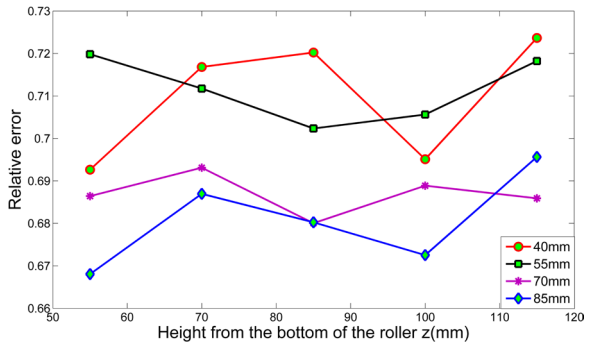

Figure 10. The relative error plot of the experimental and simulation

corresponding contact force must be different. Based on the Hertz elastic contact theory, the correction coefficient k to regard the effect of the contact material and the position of the workpiece on the actual contact force was adopted, and the correction contact pressure F calculation formula between the barrel finishing abrasive and the workpiece was proposed.

$$F = k\left(\frac{4}{3}E^*(R^*)^{1/2}\delta_n^{3/2}\right). \tag{6}$$

In the formula: k is the comprehensive correction coefficient, $k = k_1{}^* k_2$, k_1 and k_2 are the material correction coefficient and the position correction coefficient, respectively.

At present, the study of the barrel finishing process, the determination of the correction factor k and the related theoretical calculation have not been reported. The influence of the contact force of the material properties and the position of the workpiece in the contact process was quantified, and the formula for the contact force between the barrel finishing abrasive and the workpiece was deduced in this paper.

4.1 Material Correction Coefficient k_1

As there exist significant differences in the mechanical effects between the actual engineering materials and the elastic materials assumed by Hertz contact mechanics, the calculation results are often different from the actual force. Based on Hertz contact theory and Newton's

second law, the calculation formula of the contact force was proposed by He et al. [28], when the collision speed of the two objects is very small. It is found that the contact force formula based on Hertz contact mechanics is different in the material of the collision system. According to the results of Refs. [28, 29], the nominal material modification coefficient of the collision system is proposed as follows:

$$k_1^* = \frac{3\pi p_y}{\left(1280\pi E^{*4}\right)^{0.2}} V^{-0.4}. \tag{7}$$

The magnitude of the effect of the velocity terms $V^{-0.4}$ on the material correction coefficient in Eq. (7) was firstly considered in this paper. Then exports the collision speed value between the barrel finishing abrasive and the workpiece at each grid at different moments when the rotation speed is stabilized and calculates the average value. The average collision speed values between the barrel finishing abrasive and the workpiece at different positions are shown in Table 6.

Table 6. The average collision speed value between the barrel finishing media and the workpiece at different positions (m/s)

z (mm)	*x* (mm)			
	40	55	70	85
55	0.1807	0.1820	0.1921	0.2019
70	0.1858	0.1822	0.1946	0.2205
85	0.1935	0.1947	0.2008	0.2467
100	0.1950	0.2077	0.2271	0.2519
115	0.1980	0.2143	0.2329	0.2599

The influence coefficient of the contact speed terms ($V^{-0.4}$) between the barrel finishing abrasive and the workpiece in Table 6 is calculated between 1.7855 and 1.9413, taking the average is 1.8799. Consider Eq. (5) and Eq. (7), the actual contact process material correction coefficient k_1 is proposed as:

$$k_1 = \frac{5.64\pi(1.234 + 1.256\mu)Y}{\left(1280\pi E^{*4}\right)^{0.2}}. \tag{8}$$

It is known from Eq. (8), once the material of the collision system is made certain, the material correction coefficient in the calculation of the contact force is determined. The brown corundum spherical barrel finishing abrasive as the working medium with an elastic modulus of 300 GPa and a Poisson ratio of 0.21. The workpiece elastic modulus of 79–210 GPa and the yield strength of 0.21–0.25 GPa was choosed in this paper. According to the expression of the equivalent elastic modulus in Eq. (3), the equivalent elastic modulus is 65.8–130.9 GPa. The relationship curve between the material correction coefficient and the equivalent modulus is shown in Figure 11 according to Eq. (8). It can be seen from the Figure 11 that the material correction coefficient decreases with the increase of the equivalent modulus, and its value is 1.41–2.38.

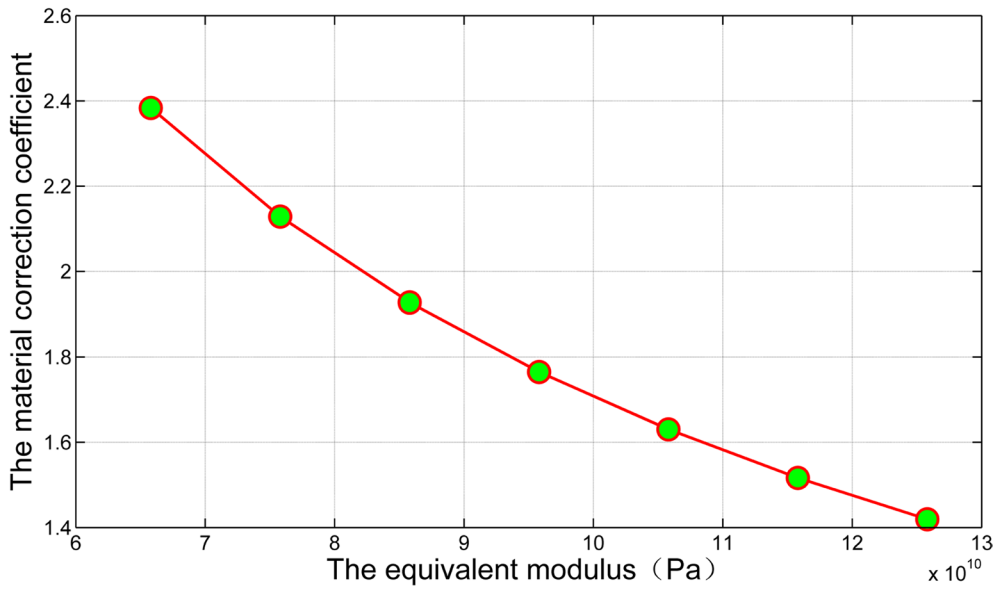

Figure 11. Curve of material correction coefficient and equivalent elastic modulus

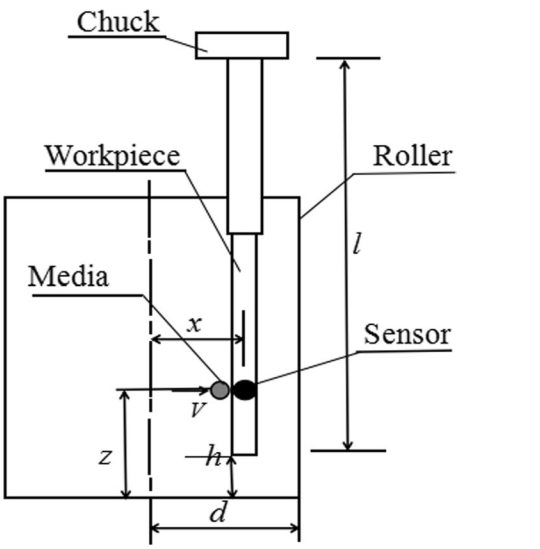

Figure 12. Collide model of abrasive and workpiece

4.2 Position Correction Coefficient

Under the interaction of the barrel finishing abrasive, different deformation responses will occur in different parts of the workpiece. Figure 12 shows the contact model between the barrel finishing abrasive and the workpiece. The fixed workpiece structure is regarded as a cantilever beam structure. According to the law of conservation of energy, the kinetic energy is converted into the strain energy of the workpiece during contact. When a fixed member is subjected to external forces, it is obtained from the Crabbey-Elron theorem and the law of conservation of energy in material mechanics. Strain energy formula for the entire workpiece [30]:

$$V_{\varepsilon l} = \int_l \frac{F_N^2(x)\mathrm{d}x}{2EA} + \int_l \frac{T^2(x)\mathrm{d}x}{2GI_p} + \int_l \frac{M^2(x)\mathrm{d}x}{2EI}. \quad (9)$$

In the barrel finishing process, the rotation of the roller drives relative movement between the abrasive and the workpiece, and the abrasive collides with the surface of the workpiece at a low speed. Considering the difference in contact force at different locations, the position correction coefficient k_2 is proposed to characterize the influence of position on contact force.

In the spindle-type barrel finishing, the fixed workpiece is subjected to the contact force of the barrel finishing medium to generate bending strain. The bending strain energy when the workpiece is fixed is derived from Eq. (9):

$$V_{\varepsilon l} = \frac{[F_N(x)]^2(l+h-z)^3}{6EI}, \quad (10)$$

where $F(x)$ is the contact force; $T(x)$ is the torque; $M(x)$ is the bending moment; I_p is the polar moment of inertia; E is the elastic modulus of the workpiece; I is the moment of inertia; h is the distance from the bottom of the workpiece to the bottom of the barrel; $F_N(x)$ is the equivalent contact force.

According to the theorem of work reciprocity, there is always an equivalent contact force that makes Eq. (11) true with the changing in radial position of the workpiece.

$$V_{\varepsilon l} = \frac{[F(x)]^2(d-x)^3}{6EI}. \quad (11)$$

Define the position correction coefficient is:

$$k_2 = a(F(x)/F_N(x))^{3\mathrm{m}/2}. \quad (12)$$

Make $b=3m/2$, then:

$$k_2 = a\left(\frac{l+h-z}{d-x}\right)^b. \quad (13)$$

The position correction factor a and b obtained by the mathematical tool MATLAB fitting. Where a and b are the values that satisfy the highest fitting degree between the surface and the corresponding point. It is obtained that $a=2.894$, $b=-0.1267$, when $l=500$ mm, $h=30$ mm, the correlation coefficient and the correction correlation coefficient respectively are $R^2=0.9673$, $R^2\mathrm{Adj}=0.9655$, and the root mean square error is $RMSE=0.02131$. The relation surface and surface fitting residual figure between the workpiece position correction coefficient and the positions of the workpieces are shown in Figure 13. The position correction coefficient of the workpiece is between 2.0 and 2.3 based on this study.

4.3 Modified Result Analysis

The universal contact force between the barrel finishing abrasive and the workpiece is obtained according to Eq. (6), Eq. (8) and Eq. (13):

$$F = \frac{5.64\pi(1.234+1.256\nu)Y}{\left(1280\pi E^{*4}\right)^{0.2}} * a\left(\frac{l+h-z}{d-x}\right)^b * \left(\frac{4}{3}E^*(R^*)^{1/2}\delta_n^{3/2}\right). \quad (14)$$

Substitute the relevant material parameters in Table 3 into Eq. (8), it is obtained that the workpiece material correction coefficient is 1.52. And by using the corrected

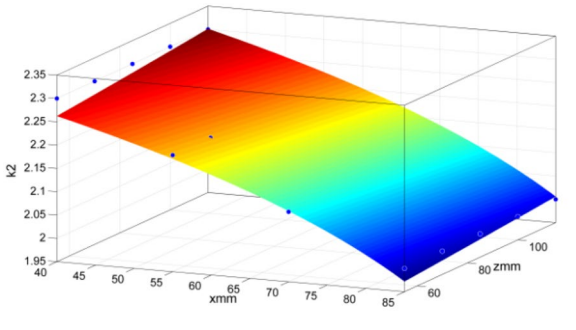

a Surface fitting

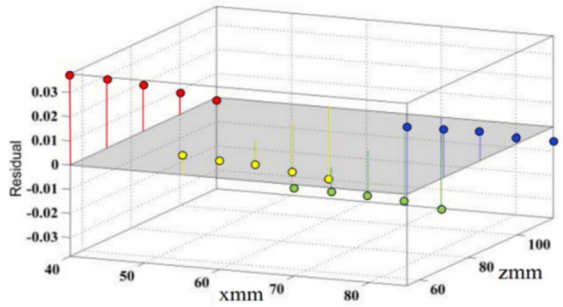

b Chart of Residuals

Figure 13. Relationship between the position correction coefficient and the position of workpiece

formula to calculate the contact force value at different positions, comparing and analyzing the simulation results with experimental results, it is found that the calculation

Table 7. Experimental results of the average normal contact force of workpiece at different positions at *v* = 60 r/min F(N)

z (mm)	*x* (mm)			
	40	55	70	85
55	2.5437	3.2318	4.8117	5.2081
70	2.1219	2.9465	3.6389	4.7393
85	1.7971	2.3384	2.8660	3.8038
100	1.0806	1.8481	2.1170	2.6938
115	0.8793	1.0213	1.1733	1.8003

Table 8. Simulation results of the average contact force of workpiece at different positions at *v* = 60 r/min F(N)

z (mm)	*x* (mm)			
	40	55	70	85
55	0.6187	0.9017	1.0938	1.5271
70	0.4418	0.8017	0.9931	1.3071
85	0.3684	0.6396	0.8503	0.9638
100	0.2915	0.4914	0.6231	0.8019
115	0.2403	0.2762	0.3328	0.5329

of the relative error is between 1.63% and 12.68%. The fitting effect of the corrected contact force calculation formula and experimental test results is shown in Figure 14.

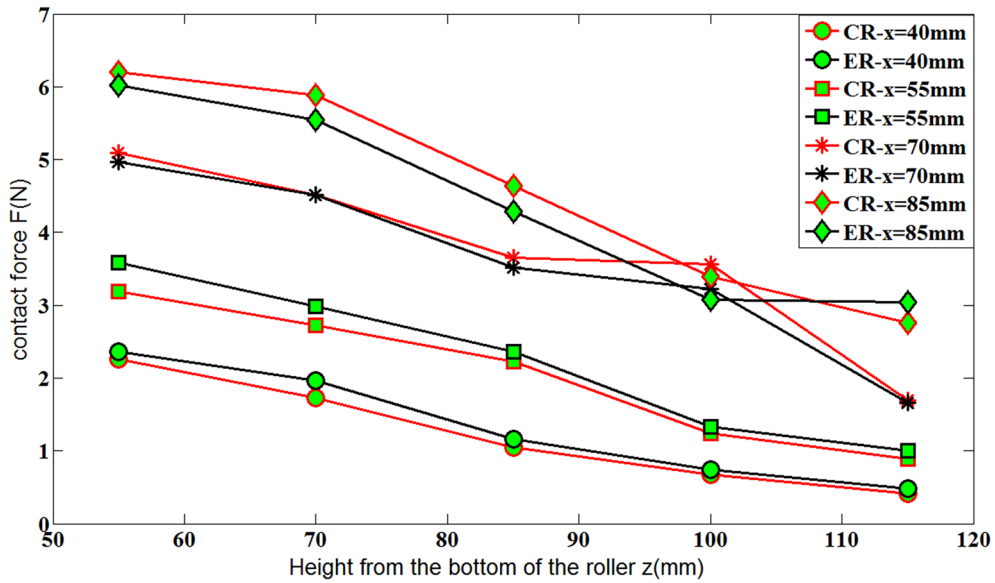

Figure 14. Comparison of calculation and experimental results of sampling points location (CR: Calculation results, ER: Experimental results)

Table 9. Calculation results of the average contact force of workpiece at different positions at $v = 60$ r/min F(N)

z (mm)	*x* (mm)			
	40	55	70	85
55	2.5023	3.5240	5.0385	5.3648
70	2.0519	2.9296	4.0565	4.9460
85	1.5754	2.2721	3.2023	4.0615
100	1.0016	1.6488	2.3406	3.0352
115	0.7766	0.9592	1.3118	1.7089

5 Experimental Verification Analysis

This paper compares and analyzes the contact force between the experimental test and the simulation at various sampling points at $v = 60$ r/min in order to check the universal suitability of the general contact force suggested above in Eq. (14). Tables 7 and 8 show the average normal contact force between the experimental test and the simulation test respectively. Table 9 shows the results of the simulation data in Table 8 calculated by Eq. (14).

Comparing the data of Tables 7 and 9 and calculating the relative error is between 0.58% and 14.07%. The result shows that the fitting effect between the corrected contact force calculation formula and experimental results is better, as shown in Figure 15.

6 Conclusions

For the spindle barrel finishing technology, this following conclusions are obtained based on the experiment and the numerical simulation.

1 In the barrel finishing process, the contact force value which is obtained based on the Hertz-Mindlin (no slip) contact model simulation is smaller than that of the actual working condition and the relative error is between 66.8% and 72.4%, so there will be a lager error when using the Hertz-MD non-slip contact model in the simulation process.
2 The average contact force between the barrel finishing abrasive and the workpiece increases with the depth of the workpiece embedded in the abrasive and the increase of the distance from the roller center shaft. It explains that the reasonable correction of the simulation contact model can effectively represent the experimental test results.
3 The material properties and the contact position of the contact system formed by the barrel finishing abrasive and the workpiece have a significant influence on the contact force. Based on Hertz elastic contact theory, after considering the material correction coefficient and the workpiece position correction coefficient, the formula for calculating the contact force between the barrel finishing abrasive and the workpiece is established and it can better reflect the actual contact condition.
4 Based on Hertz contact theory and Newton's second law, it obtains the material correction coefficient ranges from 1.41 to 2.38, which is inversely related to the equivalent modulus E and the position correction coefficient ranges from 2.0 to 2.3.
5 The contact force calculation formula is verified by changing the rotation speed. The relative error between the calculation result and the experimen-

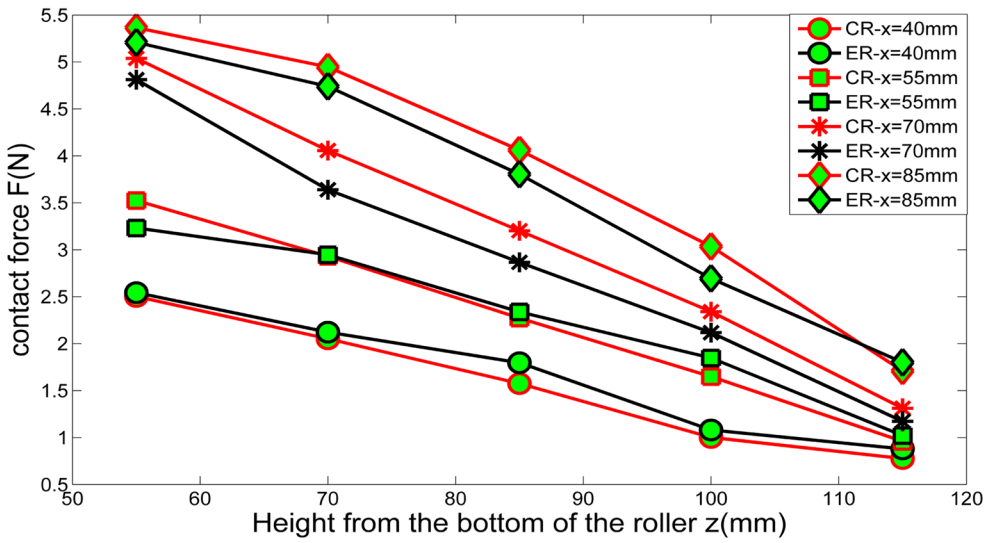

Figure 15. Comparison of calculation and experimental results of sampling points location (CR: Calculation results, ER: Experimental results)

tal test result is between 0.58% and 14.07% using the formula proposed in this paper which means the calculation result can better reflect the actual contact force. However, the influence of the size of the workpiece on the position correction expression is not considered in this paper. This will be the research direction in the future.

Acknowledgements
The authors sincerely thanks to Wenhui Li and Xiuhong Li of *Taiyuan University of Technology* for their critical discussion and reading during manuscript preparation.

Authors' Contributions
NW and BC were in charge of the whole trial; NW and SY wrote the manuscript; TZ and CW assisted with sampling and laboratory analyses. All authors read and approved the final manuscript.

Authors' Information
Na Wang, born in 1988, is currently a PhD candidate at *Shanxi Key Laboratory of Precision Machining, College of Mechanical and Vehicle Engineering, Taiyuan University of Technology, China*. She received her master degree from *Taiyuan University of Science and Technology, China*, in 2013.

Shengqiang Yang, born in 1964, is currently a professor at *Shanxi Key Laboratory of Precision Machining, College of Mechanical and Vehicle Engineering, Taiyuan University of Technology, China*. He received his PhD degree from *Taiyuan University of Technology, China*, in 2009. His research interests include surface finishing technology for precision surface.

Tingting Zhao, born in 1989, is currently a lecturer at *College of Mechanical and Vehicle Engineering, Taiyuan University of Technology, China*. She received her PhD degree from *Zienkiewicz Centre for Computational Engineering, College of Engineering, Swansea University, Bay Campus, Swansea, SA1 8EN, UK*, in 2019.

Bo Cao, born in 1993, is currently an assistant Engineer of *Hudong Depot, China*. He received his master degree from *Taiyuan University of Technology, China*, in 2019.

Chenwei Wang, born in 1992, is currently an assistant Engineer of *FAW Jiefang Automobile Co., Ltd, China*. He received his master degree from *Taiyuan University of Technology, China*, in 2019.

Funding
Supported by Program National Natural Science Foundation of China (Grant Nos. 51875389, 51975399, 52075362) and Key Program of Natural Science Foundation of Shanxi Province of China (Grant No. 201801D111002) and Scientific and Technological Innovation Project for Excellent Talents in Shanxi Province of China (Grant No. 201805D211031).

Competing Interests
The authors declare that they have no competing interests.

Author Details
[1] College of Mechanical and Vehicle Engineering, Taiyuan University of Technology, Taiyuan 030024, China. [2] Shanxi Key Laboratory of Precision Machining, Taiyuan University of Technology, Taiyuan 030024, China.

Received: 27 September 2018 Revised: 29 October 2020 Accepted: 3 November 2020
Published online: 23 November 2020

References

[1] S Q Yang. Surface finishing theory and new technology. *Springer*, 2018. https://doi.org/10.1007/978-3-662-54133-3.
[2] R Singh, A Trivedi, S Singh. Experimental investigation on shore hardness of barrel-finished FDM patterns. *Indian Academy of Sciences*, 2017, 42(9): 1579-1584. https://doi.org/10.1007/s12046-017-0709-6.
[3] A Boschetto, L Bottini, F Veniali. Surface roughness and radiusing of Ti6Al4V selective laser melting-Manufactured parts conditioned by barrel finishing. *International Journal of Advanced Manufacturing Technology*, 2018, 94: 2773-2790. https://doi.org/10.1007/s00170-017-1059-6.
[4] X H Li, F F Wu, W H Li, et al. Kinematic characteristics of mass finishing process with the parallel spindle: Velocity measurement and analysis of the media. *Advances in Mechanical Engineering*, 2017, 9(10): 1-12. https://doi.org/10.1177/1687814017729091.
[5] A Boschetto, V Gordano, F Veniali. Micro-removal modeling of surface roughness in barrel finishing. *International Journal of Advanced Manufacturing Technology*, 2013, 69: 2343-2354. https://doi.org/10.1007/s00170-013-5186-4.
[6] X H Li, W H Li, S Q Yang, et al. Experimental investigation into the surface integrity and tribological property of AISI 1045 steel specimen for barrel finishing. *Procedia CIRP*, 2018, 71: 47-52. https://doi.org/10.1016/j.procir.2018.05.021.
[7] X Z Wang, S Q Yang, W H Li, et al. Vibratory finishing co-simulation based on ADAMS-EDEM with experimental validation. *International Journal of Advanced Manufacturing Technology*, 2018, 96: 1175-1185. https://doi.org/10.1007/s00170-018-1639-0.
[8] X Z Wang, S Q Yang, W H Li, et al. Experimental investigation of adherent vibratory finishing for sheet specimens. *Surface Technology*, 2017, 46(10): 261-267. DOI:10.16490/j.cnki.issn.1001-3660.2017.10.039. (in Chinese)
[9] V Cariapa, H Park, J Kim, et al. Development of a metal removal model using spherical ceramic media in a centrifugal disk mass finishing machine. *International Journal of Advanced Manufacturing Technology*, 2008, 39: 92-106. https://doi.org/10.1007/s00170-007-1195-5.
[10] J Gong, Z Nie, Y Zhu, et al. Exploring the effects of particle shape and content of fines on the shear behavior of sand-fines mixtures via the DEM. *Computers & Geotechnics*, 2019, 106: 161-176. https://doi.org/10.1016/j.compgeo.2018.10.021.
[11] N Wang, T T Zhao, S Q Yang, et al. Experiment and simulation analysis on the mechanism of the spindle barrel finishing. International Journal of Advanced Manufacturing Technology, 2020, 109: 57-74. https://doi.org/10.1007/s00170-020-05609-y.
[12] S M Francisco, L I Jose, R C Victor. Numerical tooth contact analysis of gear transmissions through the discretization and adaptive refinement of the contact surfaces. *Mechanism and Machine Theory*, 2016, 101: 75-94. https://doi.org/10.1016/j.mechmachtheory.2016.03.009.
[13] X Z Wang, S Q Yang, W H Li, et al. Simulation and analysis of the cascade vibratory finishing based on EDEM. *Global Conference on Materials Science and Processing Technologies*, 2016: 11.
[14] N Wang, S Q Yang, T T Zhao, et al. Correction calculation on the elasto-plastic contact force of spindle barrel finishing. *Surface Technology*, 2020, 49(08): 333-341. https://doi.org/10.16490/j.cnki.issn.1001-3660.2020.08.039. (in Chinese)
[15] Z M Hao, W H Li, X H Li, et al. Effect of media parameters on contact forces in centrifugal barrel finishing. *China Science Paper*, 2017, 12(23): 2756-2760. (in Chinese)
[16] B Cao, W H Li, X H Li, et al. Calibration of discrete element parameters of the wet barrel finishing abrasive based on JKR model. *Surface Technology*, 2019, 048(003): 249-256. https://doi.org/10.16490/j.cnki.issn.1001-3660.2019.03.034. (in Chinese)
[17] Y Tian, W H Li. Crankshaft barrel finishing mechanism analysis based on the discrete element method. *Modern Manufacturing Engineering*, 2015(3): 79-83. (in Chinese)
[18] X Yan. *Theoretical analysis and simulation of the vibration system of the waterfall vibration finishing equipment*. Taiyuan: Taiyuan University of Technology, 2016. (in Chinese)
[19] C H Song. *Theoretic analysis and simulation of centrifugal barrel finishing based on three-dimensional discrete element method*. Taiyuan: Taiyuan University of Technology, 2010. (in Chinese)
[20] Y Chen. *Motion analysis of medium and numerical Simulation of horizontal centrifugal barrel finishing*. Kunming: Kunming University of Technology, 2017. (in Chinese)
[21] W H Li, L Zhang, X H Li, et al. Theoretical and simulation analysis of abrasive particles in centrifugal barrel finishing: Kinematics mechanism

and distribution characteristics. *Powder Technology*, 2017, 318, 518-527. https://doi.org/10.1016/j.powtec.2017.06.033.
[22] Y H Zhou. Modeling of soft sphere normal collisions with characteristic of restitution dependent on impact velocity. *Theoretical and Applied Mechanics Letters*, 2013, 3: 021003.
[23] T Kawaguchi, T Tanaka, Y Tsuji. Numerical simulation of two dimensional fluidized bed using the discrete element method. *Power Technology*, 1998, 96(2): 129-138. https://doi.org/10.1016/S0032-5910(97)03366-4.
[24] A P Grima, P W Wypych. Investigation into calibration of discrete element model parameters for scale-up and validation of particle-structure interactions under impact conditions. *Powder Technology*, 2011, 212: 198-209.
[25] Y N Chen, W Li, X H Li, et al. Force test and analysis of abrasive in spindle barrel finishing process. *China Surface Engineering*, 2017, 30(1): 33-40. (in Chinese)
[26] K L Johnson. Contact mechanics[J]. *Journal of Tribology*, 1985, 108(4): 464.
[27] R V Brizme, Y Kligerman, I Etsion. The effect of contact conditions and material properties on the elasticity terminus of a spherical contact. *International Journal of Solids and Structures*, 2006, 43(18/19): 5736-5749. https://doi.org/10.1016/j.ijsolstr.2005.07.034.
[28] S M He, X P Li, Y Wu. Calculation of impact force of out runner blocks in debris flow considering elastoplastic deformation. *Chinese Journal of Rock Mechanics and Engineering*, 2007, 26(8): 1664-1669. https://doi.org/10.1016/S1672-6529(07)60007-9. (in Chinese)
[29] J Chen, Q C Wang, Y Q Chen, et al. Amending calculation on impact force of boulders in debris flow based on Hertz theory. *Journal of Harbin Institute of Technology*, 2017, 49(2): 124-129. (in Chinese)
[30] D Capecchi, G Ruta. Strengh of materials and theory of elasticity in 19th century Italy. *Springer*, 2015. https://doi.org/10.1007/978-3-319-05524-4.